

REVISITING STELLAR EQUATORIAL ROTATIONAL VELOCITIES WITH GAIA DR3 LINE BROADENING—THE DEPENDENCE ON TEMPERATURE, MASS AND AGE

AMITAY SUSSHOLZ  ¹, TSEVI MAZEH  ^{1,2}, AND SIMCHON FAIGLER  ¹¹ School of Physics and Astronomy, Tel Aviv University, Tel Aviv, 6997801, Israel and² Max-Planck-Institut für Astronomie, Königstuhl 17, D-69117 Heidelberg, Germany

Version January 29, 2026

ABSTRACT

We used more than 10^5 *Gaia* DR3 line broadening `vbroad` measurements to examine stellar rotation as a function of stellar temperature, mass and age. The large sample clearly displays the Kraft break at $\sim 6,500$ K, or mass of $\sim 1.3 M_{\odot}$ —while `vbroad` are small, on the order of 10–20 km/s, for stars cooler than the Kraft break, they sharply rise above the break, reaching up ~ 100 km/s with temperature of 7,000 K. To follow the stellar rotation as a function of age, we consider `vbroad` as a function of scaled age—stellar age divided by the relevant Terminal Age Main Sequence (MS), for four narrow mass bins. We find that stellar rotation deceleration is slow during the MS phase and fast afterwards for stars hotter than the break, whereas deceleration rate is relatively high and does not vary much for the cool stars. Our findings are consistent with the theory that stellar rotation slowing is due to magnetic braking, emanating from magnetic fields that are anchored to the stellar convective envelopes. Therefore, deceleration is high in cool stars, but in hot stars only after they leave the MS and develop convective outer layers.

1. INTRODUCTION

Stellar rotation is a fundamental property of stars, intimately linked to their internal structure, angular momentum evolution, and magnetic activity (Noyes et al. 1984). Rotation influences stellar winds, dynamo efficiency, internal mixing, and ultimately affects stellar lifetimes and planetary environments (Kraft 1967; Kawaler 1987; Bouvier et al. 1997; Wolff & Simon 1997). Understanding how stars lose angular momentum across the main sequence (MS) and beyond has therefore remained a central question in stellar astrophysics for more than half a century (Weber & Davis 1967; Mestel 1968; Skumanich 1972; Bouvier et al. 2014; Lu et al. 2022; Amaral 2025).

The pioneering work of Kraft (1967) established the sharp transition in rotation rates around spectral type F, now known as the *Kraft break*. Cooler stars spin down efficiently through magnetized stellar winds, whereas hotter stars ($T_{\text{eff}} \gtrsim 6,200$ K) retain high rotation velocities due to their shallow convection zones that do not allow strong magnetic fields (e.g., Kraft 1967; Kawaler 1987; Bouvier et al. 1997; Wolff & Simon 1997). Subsequent studies refined this picture, exploring the relation between angular momentum, mass, and stellar activity (van Saders & Pinsonneault 2012, 2013; McQuillan et al. 2014; Beyer & White 2024). Furthermore, some studies even suggest that the stellar rotation might be used as a measure of stellar age for stars below the Kraft brake (e.g., Skumanich 1972; Barnes 2003, 2007; Angus et al. 2015).

With the advent of *Kepler* and *TESS*, tens of thousands of stellar rotation periods were measured from

photometric variability (Nielsen et al. 2013; McQuillan et al. 2014; Santos et al. 2019, 2021; Reinhold et al. 2023; Kamai & Perets 2025; Gao et al. 2025). These studies revealed complex rotation-period distributions, strong mass dependencies, and evidence for weakened magnetic braking at old stellar ages (van Saders et al. 2013; Matt et al. 2015; van Saders et al. 2016; Avallone et al. 2022).

However, photometric methods inherently suffer from several drawbacks (see recent discussion by Binnenfeld et al., 2026, submitted). Rotation periods can only be detected when stars display surface inhomogeneities such as spots, which are often absent or evolve rapidly (Aigrain et al. 2015). Measured periods may also correspond to spot evolution timescales or harmonics rather than the true stellar rotation rate, introducing some biases (Reinhold et al. 2013; McQuillan et al. 2014). Furthermore, old and slowly rotating stars tend to exhibit weak variability, leading to strong selection effects against long-period rotators [e.g., η (Metcalfe et al. 2016)]. These limitations motivate complementary approaches based on spectroscopy, where projected rotational velocities, derived from the broadening of the absorption lines, provide an independent tracer of stellar rotation, albeit with unknown stellar rotational inclination.

Admittedly, spectroscopic measurements can be affected by other sources of line broadening, most notably macroturbulence, which may bias the inferred rotational velocity (e.g., Gray 2005; Doyle et al. 2014). Moreover, deriving stellar rotation periods from spectroscopic measurements requires knowledge of the stellar radius, introducing further uncertainties. Nevertheless, the *Gaia* revolution, that made millions of stellar spectra available,

provides a powerful complementary avenue to photometric studies of stellar rotation.

The *Gaia* space mission carries a spectrometer with intermediate resolving power $R \approx 11,500$, covering the 846–870 nm wavelength range, with the primary goal of measuring radial velocities (RVs) for bright sources (Cropper et al. 2018; Sartoretti et al. 2022), down to magnitude $G_{\text{RVS}} \sim 16$ (Katz et al. 2023). The spectroscopic pipeline (Sartoretti et al. 2018) also derives a line-broadening parameter, estimating the broadening of absorption lines relative to template spectra, producing `vbroad` values for 3,524,677 sources in *Gaia* DR3 (Frémat et al. 2023).

This parameter, while not a direct measurement of projected rotational velocity ($v \sin i$), provides an important statistical tracer of stellar rotation. Although the relatively low resolution of the *Gaia* spectra limits the `vbroad` precision, the unprecedented large number of measurements opens new avenues of research (e.g., Hadad et al. 2025b,a), which was not possible before. This potential is further enhanced by the availability of stellar radii and masses from *Gaia* (Gaia Collaboration et al. 2023; Andrae et al. 2023; Creevey et al. 2023) for this exceptionally large sample.

In this work, we used *Gaia* DR3 measurements to explore the distribution of projected rotation and specific angular momentum across the MS and beyond, with particular emphasis on stars below and above the Kraft break. We construct a color-magnitude diagram to exclude giant stars from our sample, and examine the dependence of *Gaia* `vbroad` on stellar mass and age. Our analysis highlights the distinct rotational behaviors above and below the Kraft break and provides new empirical constraints on models of angular momentum evolution.

In Section 2 we describe the *Gaia* DR3 `vbroad` sample, the applied quality cuts, and the construction of a clean main-sequence (MS) subset, including our use of FLAME masses and ages and the age-scaling relative to an interpolated terminal-age MS. In Section 3 we present the distribution of `vbroad` as a function of effective temperature and mass, reproducing the break seen in Kraft’s original paper. In Section 4 we examine the evolution of `vbroad` and the derived specific angular momentum as a function of scaled age in narrow mass bins, contrasting stars above and below the Kraft break. Finally, we discuss the implications of our results and dominant sources of uncertainty in Section 5.

2. DATA SELECTION

We base our analysis on 3,524,677 line-broadening measurements (`vbroad`) published in *Gaia* Data Release 3 (Frémat et al. 2023). We used ADQL queries via the Table Access Protocol (TAP)¹ service (Salgado et al. 2017) to retrieve data from the *Gaia* DR3 source catalog (Gaia Collaboration et al. 2023). Stellar parameters from GSP-Phot (e.g., `teff_gspphot`, `radius_gspphot`) were taken from Andrae et al. (2023), and evolutionary parameters from FLAME (e.g. `mass_flame`, `age_flame`) were taken from the CU8/Apsis DR3 products (Creevey et al. 2023).

¹ <https://www.star.bris.ac.uk/mbt/topcat/sun253/TapTableLoadDialog.html>

To ensure reliable and astrophysically meaningful measurements, we applied the following quality cuts:

- `vbroad_error < max(10, 0.5 * vbroad)`: we require a detection significance of at least 2σ to exclude poorly constrained broadening measurements, which could otherwise bias the inferred rotation distribution, but allowing for near zero values.
- $4,000 \text{ K} < T_{\text{eff, GSPphot}} < 8,000 \text{ K}$: this range selects FGK MS stars, covering the cool dwarf regime and extending up to early F-type stars above the Kraft break.
- $\varpi/\sigma_{\varpi} > 10$: accurate distances are essential to compute reliable absolute magnitudes and radii. This cut removes stars with poorly constrained parallaxes, minimizing contamination in the CMD (Gaia Collaboration et al. 2018).
- $R_{\text{GSPphot}}/\sigma_{R, \text{lower}} > 5$: we retain only stars with well-determined radii, ensuring that subsequent calculations of angular momentum are robust.
- $M_{\text{FLAME}}/\sigma_{M, \text{lower}} > 5$: similarly, we require well-determined stellar masses from the *Gaia* FLAME module.

After these cuts, our working sample contained 1,300,637 stars, of which 1,116,716 have an age value in FLAME.

To further restrict the sample to MS stars, we constructed a color-magnitude diagram (CMD) using extinction-corrected *Gaia* photometry. To isolate MS stars, including mildly evolved ones, we defined a scaled evolutionary age as the ratio of the FLAME age to the corresponding terminal-age main sequence (TAMS), $t_{\text{FLAME}}/T_{\text{AMS}}$. The TAMS values were defined following van Saders & Pinsonneault (2013) as the age at which the central hydrogen abundance satisfies $\chi_c < 2 \times 10^{-4}$.

To compute TAMS as a function of stellar mass, we downloaded the “`fastlaunch_full.tar.gz`” and “`slowlaunch_full.tar.gz`” grids from Clayton et al. (2025) using the `kiauhoku`² package (Clayton et al. 2020) based on YREC models at solar metallicity. These grids were used to construct a lookup table of stellar masses and their corresponding TAMS values. For stars with masses in the range $0.68 \leq M/M_{\odot} \leq 2$, we interpolated the TAMS using a Piecewise Cubic Hermite Interpolating Polynomial (PCHIP)³. For masses outside this range, we extrapolated the TAMS values using a power-law fit.

To avoid over culling our data and account for inaccuracies in the values of FLAME’s ages, we decided to include slightly evolved stars with $t_{\text{FLAME}}/T_{\text{AMS}} \leq 1.2$. The final sample selection was performed through visual inspection of the stellar locations in the CMD, using $t_{\text{FLAME}}/T_{\text{AMS}}$ as a color-coded guide, as illustrated in Figure 1. This cut effectively removes evolved stars, yielding a MS sample of 424,270 stars for our subsequent analysis of stellar rotation and angular momentum. Focusing on the main bulk of our MS sample, we further restrict the data to stars with $0.8 \leq M/M_{\odot} \leq 1.7$ and $4,800 \text{ K} \leq T_{\text{eff}} \leq 7,800 \text{ K}$, resulting in a final sample of 354,849 stars.

² <https://zenodo.org/records/14908017>

³ <https://www.mathworks.com/help/matlab/ref/pchip.html>

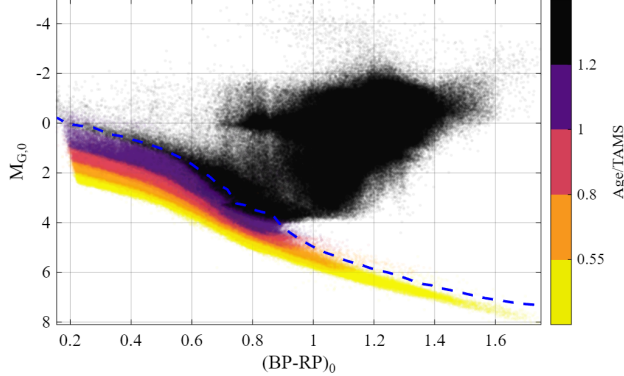


FIG. 1.— Extinction-corrected *Gaia* CMD of 1,116,716 stars sample with reliable v_{broad} measurements from *Gaia* DR3, and an Age value in FLAME. Point density is presented via point alpha value, colored by the stars' evolutionary stage (Age/TAMS) in 5 discrete ranges. The dashed blue curve was used to separate the MS from evolved stars. Stars below the curve are the final clean MS sample used in this work (424,270 stars).

3. VBROAD AS A FUNCTION OF TEMPERATURE

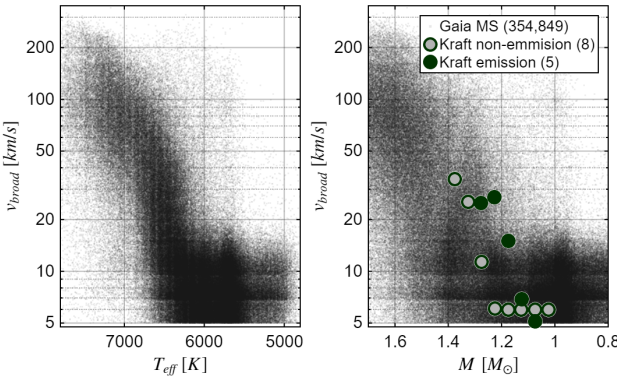


FIG. 2.— *Left*: Projected rotational velocity (v_{broad}) versus effective temperature, taken from *Gaia* GSPhot. Hotter stars tend to rotate more rapidly as presented here. *Right*: Projected rotational velocity (v_{broad}) versus stellar mass, taken from *Gaia* FLAME for 354,849 *Gaia* MS stars. Filled and open circles are data points taken from Fig 3. of Kraft (1967).

Figure 2 displays v_{broad} values as a function of stellar effective temperature and mass. The Kraft break is clearly seen. For $T_{\text{eff}} \lesssim 6,250$ K ($M \lesssim 1,3-1,4 M_{\odot}$) the rotational velocities are mostly less than ~ 10 km/s, which is below the resolution of *Gaia* RVS. Beyond this range, we see a strong rise of v_{broad} as a function of temperature or mass.

We overplotted the thirteen measurements of Kraft (1967) on the figure. Remarkably, the trend identified by Kraft, based on only 13 stars, is fully confirmed by the *Gaia* v_{broad} measurements of several hundred thousand stars.

4. VBROAD AND SPECIFIC ANGULAR MOMENTUM AS A FUNCTION OF AGE

Figure 2 shows a pronounced dependence of v_{broad} on stellar mass and effective temperature with a large scatter, likely driven by the wide range of stellar ages in the sample. To study the dependence on stellar age, we plot in Figure 3 v_{broad} as a function of stellar age for four slices of masses.

We scaled the age by the TAMS, so age of unity corresponds to the transition of the star from its MS phase to the relatively fast expansion phase. By construction, the figure extends up to a scaled age of 1.25, allowing the rotational-velocity evolution to be traced beyond the end of the MS phase.

In order to follow the stellar angular momentum loss we plotted in the lower panel of the figure the stellar specific angular momentum (SAM) as a function of their age, with the same mass bins. The SAM of each star was derived by multiplying its equatorial rotational velocity v_{broad} by its FLAME radius.

Figure 3 displays a significant difference in the age-dependence pattern of v_{broad} and SAM for stars below and above the Kraft break. Stars above the Kraft break, with 1.5 and $1.6 M_{\odot}$, display a slow rate of deceleration of their rotational velocity and their SAM at their MS phase, and then change into a much faster rate as they evolve off the main sequence. In contrast, stars with masses below the Kraft break show opposite behavior—fast deceleration of stellar rotation and SAM during the main sequence and much slower deceleration at the post-MS phase.

5. DISCUSSION

We used more than 10^5 *Gaia* v_{broad} measurements to examine the deceleration of stellar rotation as stars evolve along and beyond the main sequence. The analysis is affected by two main sources of uncertainty. The first concerns the derivation of stellar equatorial rotational velocities. The medium spectral resolution of *Gaia* introduces relatively large v_{broad} uncertainties, of the order of 10 km/s, such that values below ~ 20 km/s are likely not robust. The v_{broad} measurements are also affected by additional broadening effects, such as macro-turbulence, which tend to increase the inferred values (Frémant et al. 2023), while the unknown inclination leads to an overall underestimation of the true equatorial velocity (e.g., Hadad et al. 2025b,a). Finally, the limited wavelength coverage of the RVS spectra and their center in the red part of the spectrum limit the ability to derive equatorial rotational velocities.

The second source of uncertainty is associated with the stellar parameters—effective temperature, radius, mass, and age, adopted from the FLAME catalog (Creevey et al. 2023). While the stellar radius and effective temperature are derived directly from *Gaia* photometry and parallax (Gaia Collaboration et al. 2023), the stellar mass—and especially the age—are strongly model dependent (Fouesneau et al. 2023). Despite these limitations, the large size of the sample allows clear and statistically robust patterns of stellar rotation evolution to emerge.

We therefore focus on the equatorial rotational velocities and do not consider the stellar rotation periods, in order to avoid the need to divide the v_{broad} values by the stellar radii, which would introduce an additional uncertainty. Nevertheless, when considering the specific angular momentum, we had no choice but to multiply v_{broad} by the stellar radius.

The large sample clearly reveals the Kraft break at $\sim 6,500$ K, corresponding to a mass of $\sim 1.3 M_{\odot}$. Stars cooler than the Kraft break exhibit low v_{broad} , typically of order 10–20 km/s. For stars above the break, equatorial velocities rise steeply as a function of temperature,

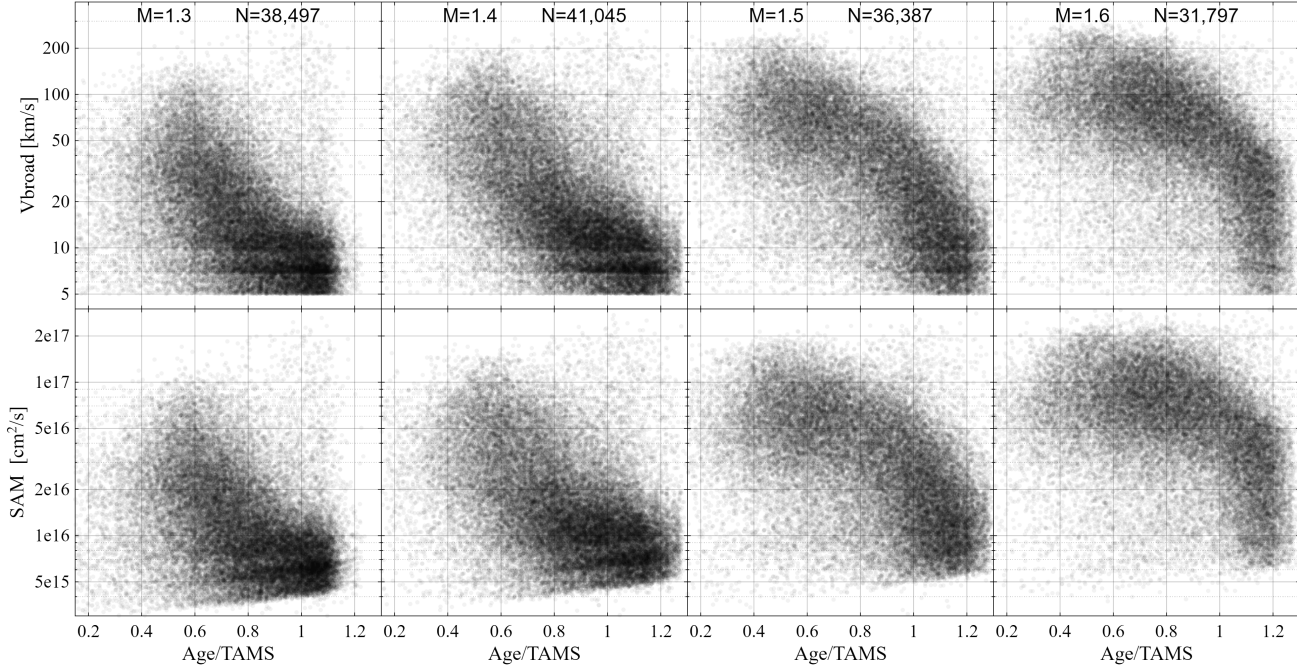


FIG. 3.— *Upper:* Stellar Gaia’s v_{broad} vs. the corresponding GSP-Phot’s evolutionary stage in four FLAME-mass bins, with width of $0.1 M_{\odot}$. Bin centers are at $1.3 M_{\odot}$, $1.4 M_{\odot}$, $1.5 M_{\odot}$ and $1.6 M_{\odot}$. We use *Gaia* scaled age—defined as the stellar age in units of the stellar interpolated TAMS (see text). Our distributions are plotted as translucent black dots, signifying point density. *Lower:* The stellar specific angular momentum vs. its scaled age.

up to ~ 100 km/s for stars with $T_{\text{eff}} \sim 7,000$ K.

The dependence of v_{broad} on stellar mass and effective temperature displays a large scatter, likely driven by the wide range of stellar ages in the sample. To trace stellar rotation as a function of age, we examine v_{broad} in four narrow mass bins, spanning both sides of the Kraft break. For each star, we used the scaled age—defined as the stellar age divided by the corresponding terminal-age MS (TAMS) age (see a similar approach in Sun & Chiappini 2024). We find distinctly different patterns of equatorial-velocity variability for stars above and below the break. For stars hotter than the break, stellar rotation deceleration is slow during the MS phase, but increases rapidly after MS departure. For cooler stars below the break, the deceleration rate is relatively high and varies only weakly with evolutionary stage.

We also present the stellar specific angular momentum as a function of the scaled age, derived from the observed equatorial rotational velocities and the stellar radii. However, a cautionary note is due here. Although the derivation accounts for variations in stellar radius, it assumed a constant radius of gyration for all ages and for all stars, which is clearly an oversimplification. This approximation may be adequate during the MS phase, but it becomes increasingly unrealistic after MS departure, when rapid stellar expansion dramatically alters the internal density profile. Nevertheless, the derived SAM follows the same qualitative trends as the equatorial velocities, indicating rapid angular-momentum loss whenever the stellar envelope is convective. The detailed evolution of angular-momentum loss after MS departure remains to be explored.

Our findings are consistent with the theoretical picture in which stellar spin-down is driven by magnetic braking associated with magnetic fields anchored in convective

envelopes (see the recent review by Aerts 2025). Consequently, rotational deceleration is strong in cool stars with deep convective envelopes, and in hotter stars only after they leave the MS and develop convective outer layers. However, a detailed quantitative confrontation between theory and the statistical properties of stellar rotation still awaits larger and more homogeneous datasets.

Gaia spectra are obviously not the only source for deriving stellar rotation. The LAMOST database (Liu et al. 2020), for example, has been used by Sun & Chiappini (2024) to derive stellar parameters, including rotation periods, for $\sim 10^5$ stars. Another major multi-object project is GALAH (Buder et al. 2021, 2025), which has yielded nearly a million rotational velocities (e.g., Das et al. 2025). In the near future, ongoing and upcoming multi-object spectroscopic surveys will continue to produce large numbers of high-quality spectra, including the upcoming 4MOST project (de Jong et al. 2019, 2022), and *Gaia* DR4,⁴ expected at the end of 2026, which will release many more v_{broad} determinations.

The complementary approach of deriving stellar rotation periods from photometric variability will also provide a wealth of additional rotation measurements. The *Gaia* rotation module (Distefano et al. 2023) is expected to deliver a large number of stellar rotation periods based on *Gaia* photometry. Within the next few years, the *PLATO* space mission (Rauer et al. 2025) will further expand this effort by producing many stellar light curves that enable robust rotation-period determinations.

A comprehensive study that integrates all available datasets into a coherent picture of stellar rotation as a function of stellar parameters—especially age—is still needed. This includes stellar rotation of stars in open

⁴ <https://www.cosmos.esa.int/web/gaia/data-release-4>

clusters (e.g., Prosser et al. 1995; Meibom & Mathieu 2005; Meibom et al. 2015; Fritzewski et al. 2021), where we know the stellar age quite well, and extension of the analysis to early-type (e.g., Ramírez-Agudelo et al. 2015; Blex et al. 2024) and metal-poor stars (Mokiem et al. 2006). Such a study will also need to confirm or refute unexpected features, such as the non-monotonic behavior of A-star rotational velocities reported by Sun & Chiappini (2024), which is not observed in our analysis. Sun & Chiappini (2024) also found a stellar rotation metallicity

dependence, which should be followed carefully for stars of different masses.

A comprehensive picture of stellar rotational evolution will ultimately allow a quantitative determination of angular-momentum loss rates and their dependence on stellar properties (see the seminal work of Mestel 1968). Ultimately, this will enable refinement of the gyrochronology techniques (Barnes 2007, 2010; Aerts 2025), allowing more accurate age determinations based on stellar mass and rotation.

REFERENCES

Aerts, C. 2025, A&A, 704, A332, doi: [10.1051/0004-6361/202556794](https://doi.org/10.1051/0004-6361/202556794)

Aigrain, S., Llama, J., Ceillier, T., et al. 2015, MNRAS, 450, 3211, doi: [10.1093/mnras/stv853](https://doi.org/10.1093/mnras/stv853)

Amaral, J. H. 2025, <https://repositorio-aberto.up.pt/bitstream/10216/169128/2/737138.pdf>

Andrae, R., Fouesneau, M., Sordo, R., et al. 2023, A&A, 674, A27, doi: [10.1051/0004-6361/202243462](https://doi.org/10.1051/0004-6361/202243462)

Angus, R., Aigrain, S., Foreman-Mackey, D., & McQuillan, A. 2015, MNRAS, 450, 1787, doi: [10.1093/mnras/stv423](https://doi.org/10.1093/mnras/stv423)

Avallone, E. A., Tayar, J. N., van Saders, J. L., et al. 2022, ApJ, 930, 7, doi: [10.3847/1538-4357/ac60a1](https://doi.org/10.3847/1538-4357/ac60a1)

Barnes, S. A. 2003, ApJ, 586, 464, doi: [10.1086/367639](https://doi.org/10.1086/367639)

—. 2007, ApJ, 669, 1167, doi: [10.1086/519295](https://doi.org/10.1086/519295)

—. 2010, ApJ, 722, 222, doi: [10.1088/0004-637X/722/1/222](https://doi.org/10.1088/0004-637X/722/1/222)

Beyer, A., & White, R. 2024, in American Astronomical Society Meeting Abstracts, Vol. 243, American Astronomical Society Meeting Abstracts #243, 205.08

Blex, S., Haas, M., & Chini, R. 2024, A&A, 692, A192, doi: [10.1051/0004-6361/202450176](https://doi.org/10.1051/0004-6361/202450176)

Bouvier, J., Forestini, M., & Allain, S. 1997, A&A, 326, 1023

Bouvier, J., Matt, S. P., Mohanty, S., et al. 2014, in Protostars and Planets VI, ed. H. Beuther, R. S. Klessen, C. P. Dullemond, & T. Henning, 433–450, doi: [10.2458/azu_uapress_9780816531240-ch019](https://doi.org/10.2458/azu_uapress_9780816531240-ch019)

Buder, S., Sharma, S., Kos, J., et al. 2021, MNRAS, 506, 150, doi: [10.1093/mnras/stab1242](https://doi.org/10.1093/mnras/stab1242)

Buder, S., Kos, J., Wang, X. E., et al. 2025, PASA, 42, e051, doi: [10.1017/pasa.2025.26](https://doi.org/10.1017/pasa.2025.26)

Claytor, Z. R., Tayar, J., & Morales, L. 2025, KIAUHOKU Stellar Evolutionary Model Grids, 2.1.2, Zenodo, doi: [10.5281/zenodo.14908017](https://doi.org/10.5281/zenodo.14908017)

Claytor, Z. R., van Saders, J. L., Santos, A. R. G., et al. 2020, kiauhoku: Stellar model grid interpolation, Astrophysics Source Code Library, record ascl:2011.027. <http://ascl.net/2011.027>

Creevey, O. L., Sordo, R., Pailler, F., et al. 2023, A&A, 674, A26, doi: [10.1051/0004-6361/202243688](https://doi.org/10.1051/0004-6361/202243688)

Cropper, M., Katz, D., Sartoretti, P., et al. 2018, A&A, 616, A5, doi: [10.1051/0004-6361/201832763](https://doi.org/10.1051/0004-6361/201832763)

Das, P. B., Zucker, D. B., De Silva, G. M., et al. 2025, MNRAS, 538, 605, doi: [10.1093/mnras/staf169](https://doi.org/10.1093/mnras/staf169)

de Jong, R. S., Agertz, O., Berbel, A. A., et al. 2019, The Messenger, 175, 3, doi: [10.18727/0722-6691/5117](https://doi.org/10.18727/0722-6691/5117)

de Jong, R. S., Bellido-Tirado, O., Brynnel, J. G., et al. 2022, in Society of Photo-Optical Instrumentation Engineers (SPIE) Conference Series, Vol. 12184, Ground-based and Airborne Instrumentation for Astronomy IX, ed. C. J. Evans, J. J. Bryant, & K. Motohara, 1218414, doi: [10.1117/12.2628965](https://doi.org/10.1117/12.2628965)

Distefano, E., Lanzafame, A. C., Brugallera, E., et al. 2023, A&A, 674, A20, doi: [10.1051/0004-6361/202244178](https://doi.org/10.1051/0004-6361/202244178)

Doyle, A. P., Davies, G. R., Smalley, B., Chaplin, W. J., & Elsworth, Y. 2014, MNRAS, 444, 3592, doi: [10.1093/mnras/stu1692](https://doi.org/10.1093/mnras/stu1692)

Fouesneau, M., Frémat, Y., Andrae, R., et al. 2023, A&A, 674, A28, doi: [10.1051/0004-6361/202243919](https://doi.org/10.1051/0004-6361/202243919)

Frémat, Y., Royer, F., Marchal, O., et al. 2023, A&A, 674, A8, doi: [10.1051/0004-6361/202243809](https://doi.org/10.1051/0004-6361/202243809)

Fritzewski, D. J., Barnes, S. A., James, D. J., & Strassmeier, K. G. 2021, A&A, 652, A60, doi: [10.1051/0004-6361/202140894](https://doi.org/10.1051/0004-6361/202140894)

Gaia Collaboration, Babusiaux, C., van Leeuwen, F., et al. 2018, A&A, 616, A10, doi: [10.1051/0004-6361/201832843](https://doi.org/10.1051/0004-6361/201832843)

Gaia Collaboration, Arenou, F., Babusiaux, C., et al. 2023, A&A, 674, A34, doi: [10.1051/0004-6361/202243782](https://doi.org/10.1051/0004-6361/202243782)

Gao, X., Chen, X., Wang, S., & Liu, J. 2025, ApJS, 276, 57, doi: [10.3847/1538-4365/ad9dd6](https://doi.org/10.3847/1538-4365/ad9dd6)

Gray, D. F. 2005, The Observation and Analysis of Stellar Photospheres, doi: [10.1017/CBO9781316036570](https://doi.org/10.1017/CBO9781316036570)

Hadad, E., Mazeh, T., & Faigler, S. 2025a, arXiv e-prints, arXiv:2508.05774, doi: [10.48550/arXiv.2508.05774](https://doi.org/10.48550/arXiv.2508.05774)

Hadad, E., Mazeh, T., Faigler, S., & Brown, A. G. A. 2025b, A&A, 693, A214, doi: [10.1051/0004-6361/202452683](https://doi.org/10.1051/0004-6361/202452683)

Kamai, I., & Perets, H. B. 2025, AJ, 169, 59, doi: [10.3847/1538-3881/ad99ab](https://doi.org/10.3847/1538-3881/ad99ab)

Katz, D., Sartoretti, P., Guerrier, A., et al. 2023, A&A, 674, A5, doi: [10.1051/0004-6361/202244220](https://doi.org/10.1051/0004-6361/202244220)

Kawaler, S. D. 1987, PASP, 99, 1322, doi: [10.1086/132120](https://doi.org/10.1086/132120)

Kraft, R. P. 1967, ApJ, 150, 551, doi: [10.1086/149359](https://doi.org/10.1086/149359)

Liu, C., Fu, J., Shi, J., et al. 2020, arXiv e-prints, arXiv:2005.07210, doi: [10.48550/arXiv.2005.07210](https://doi.org/10.48550/arXiv.2005.07210)

Lu, Y. L., Curtis, J. L., Angus, R., David, T. J., & Hattori, S. 2022, AJ, 164, 251, doi: [10.3847/1538-3881/ac9bee](https://doi.org/10.3847/1538-3881/ac9bee)

Matt, S. P., Brun, A. S., Baraffe, I., Bouvier, J., & Chabrier, G. 2015, ApJ, 799, L23, doi: [10.1088/2041-8205/799/2/L23](https://doi.org/10.1088/2041-8205/799/2/L23)

McQuillan, A., Mazeh, T., & Aigrain, S. 2014, ApJS, 211, 24, doi: [10.1088/0067-0049/211/2/24](https://doi.org/10.1088/0067-0049/211/2/24)

Meibom, S., Barnes, S. A., Platais, I., et al. 2015, Nature, 517, 589, doi: [10.1038/nature14118](https://doi.org/10.1038/nature14118)

Meibom, S., & Mathieu, R. D. 2005, ApJ, 620, 970, doi: [10.1086/427082](https://doi.org/10.1086/427082)

Mestel, L. 1968, MNRAS, 138, 359, doi: [10.1093/mnras/138.3.359](https://doi.org/10.1093/mnras/138.3.359)

Metcalfe, T. S., Egeland, R., & van Saders, J. 2016, ApJ, 826, L2, doi: [10.3847/2041-8205/826/1/L2](https://doi.org/10.3847/2041-8205/826/1/L2)

Mokiem, M. R., de Koter, A., Evans, C. J., et al. 2006, A&A, 456, 1131, doi: [10.1051/0004-6361:20064995](https://doi.org/10.1051/0004-6361:20064995)

Nielsen, M. B., Gizon, L., Schunker, H., & Karoff, C. 2013, in Astronomical Society of the Pacific Conference Series, Vol. 479, Progress in Physics of the Sun and Stars: A New Era in Helio- and Asteroseismology, ed. H. Shibahashi & A. E. Lynas-Gray, 137, doi: [10.48550/arXiv.1503.09042](https://doi.org/10.48550/arXiv.1503.09042)

Noyes, R. W., Hartmann, L. W., Baliunas, S. L., Duncan, D. K., & Vaughan, A. H. 1984, ApJ, 279, 763, doi: [10.1086/161945](https://doi.org/10.1086/161945)

Prosser, C. F., Shetrone, M. D., Dasgupta, A., et al. 1995, PASP, 107, 211, doi: [10.1086/133541](https://doi.org/10.1086/133541)

Ramírez-Agudelo, O. H., Sana, H., de Mink, S. E., et al. 2015, A&A, 580, A92, doi: [10.1051/0004-6361/201425424](https://doi.org/10.1051/0004-6361/201425424)

Rauer, H., Aerts, C., Cabrera, J., et al. 2025, Experimental Astronomy, 59, 26, doi: [10.1007/s10686-025-09985-9](https://doi.org/10.1007/s10686-025-09985-9)

Reinhold, T., Reiners, A., & Basri, G. 2013, A&A, 560, A4, doi: [10.1051/0004-6361/201321970](https://doi.org/10.1051/0004-6361/201321970)

Reinhold, T., Shapiro, A. I., Solanki, S. K., & Basri, G. 2023, A&A, 678, A24, doi: [10.1051/0004-6361/202346789](https://doi.org/10.1051/0004-6361/202346789)

Salgado, J., González-Núñez, J., Gutiérrez-Sánchez, R., et al. 2017, Astronomy and Computing, 21, 22, doi: [10.1016/j.ascom.2017.08.002](https://doi.org/10.1016/j.ascom.2017.08.002)

Santos, A. R. G., Breton, S. N., Mathur, S., & García, R. A. 2021, ApJS, 255, 17, doi: [10.3847/1538-4365/ac033f](https://doi.org/10.3847/1538-4365/ac033f)

Santos, A. R. G., García, R. A., Mathur, S., et al. 2019, ApJS, 244, 21, doi: [10.3847/1538-4365/ab3b56](https://doi.org/10.3847/1538-4365/ab3b56)

Sartoretti, P., Blomme, R., David, M., & Seabroke, G. 2022, Gaia DR3 documentation Chapter 6: Spectroscopy, Gaia DR3 documentation, European Space Agency; Gaia Data Processing and Analysis Consortium. Online at iA href="https://gea.esac.esa.int/archive/documentation/GDR3/index.html" id="6">

Sartoretti, P., Katz, D., Cropper, M., et al. 2018, A&A, 616, A6, doi: [10.1051/0004-6361/201832836](https://doi.org/10.1051/0004-6361/201832836)

Skumanich, A. 1972, ApJ, 171, 565, doi: [10.1086/151310](https://doi.org/10.1086/151310)

Sun, W., & Chiappini, C. 2024, A&A, 689, A141, doi: [10.1051/0004-6361/202450628](https://doi.org/10.1051/0004-6361/202450628)

van Saders, J., Pinsonneault, M. H., Garcia, R. A., Mathur, S., & Metcalfe, T. S. 2013, in American Astronomical Society Meeting Abstracts, Vol. 221, American Astronomical Society Meeting Abstracts #221, 301.06

van Saders, J. L., Ceillier, T., Metcalfe, T. S., et al. 2016, Nature, 529, 181, doi: [10.1038/nature16168](https://doi.org/10.1038/nature16168)

van Saders, J. L., & Pinsonneault, M. H. 2012, ApJ, 746, 16, doi: [10.1088/0004-637X/746/1/16](https://doi.org/10.1088/0004-637X/746/1/16)

—. 2013, ApJ, 776, 67, doi: [10.1088/0004-637X/776/2/67](https://doi.org/10.1088/0004-637X/776/2/67)

Weber, E. J., & Davis, Jr., L. 1967, ApJ, 148, 217,
doi: [10.1086/149138](https://doi.org/10.1086/149138)
Wolff, S., & Simon, T. 1997, PASP, 109, 759, doi: [10.1086/133942](https://doi.org/10.1086/133942)

This paper was built using the Open Journal of Astrophysics L^AT_EX template. The OJA is a journal which

provides fast and easy peer review for new papers in the astro-ph section of the arXiv, making the reviewing process simpler for authors and referees alike. Learn more at <http://astro.theoj.org>.